Journal of Advanced Ceramics
2012, 1(3): 221-226
DOI: 10.1007/s40145-012-0025-x ISSN 2226-4108

Research Article

Complex impedance properties of $LiSr_2Nb_5O_{15}$ ceramic

N.K. MOHANTY[a], S.K. SATPATHY[a], Banarji BEHERA[a,*], P. NAYAK[a], R.N.P. CHOUDHARY[b]

[a]*School of Physics, Materials Research Laboratory, Sambalpur University, Jyoti Vihar, Burla-768 019, Odisha, India*
[b]*Department of Physics, ITER, S.O.A. University, Bhubaneswar-751 030, Odisha, India*

Received August 20, 2012; Accepted October 4, 2012
© The Author(s) 2012. This article is published with open access at Springerlink.com

Abstract: The polycrystalline sample of $LiSr_2Nb_5O_{15}$ (LSN) was prepared by a high-temperature solid state reaction technique. The impedance parameters were studied using an impedance analyzer in a wide range of frequencies (10^2-10^6 Hz) at different temperatures (28-500 ℃). Nyquist plot reveals the presence of bulk effect only. The bulk resistance of the compound decreases with rise in temperature which shows the negative temperature coefficient of resistance (NTCR) like a semiconductor. The ac conductivity spectrum was found to obey Jonscher's universal power law. DC conductivity (bulk) with temperature demonstrates that the compound exhibits Arrhenius type of electrical conductivity and the activation energy found to be 0.97 eV.

Key words: niobates; conductivity; complex impedance; modulus

1 Introduction

Ceramics with filled tungsten bronze (TB) structure [1] have received much scientific and technological attention due to their interesting dielectric, ferroelectric, pyroelectric, piezoelectric and nonlinear optic properties which have been used for various electronic devices applications such as capacitors, actuators, pyroelectric detectors, transducers, electro-optic, ferroelectrics random access memory [2-6]. The general chemical formula for TB type compound is $[(A_1)_2(A_2)_4(C)_4][(B_1)_2(B_2)_8]O_{30}$, where A-sites are occupied by mono or trivalent cations, B-sites are occupied by penta or hexavalent ions and C-sites are being small, often remains vacant or may be filled by mono or divalent cations. The distribution of metal cations in different atomic sites of TB structure plays a vital role in tailoring the physical and electrical properties of the materials for device applications. Among many ferroelectric oxides, significant work has been focused on the study of TB type ferroelectric niobates and tantalates [7-12] due to their high dielectric constant and low loss. A number of TB type compounds have been reported by Behera *et al.* [13-15] with interesting properties by the substitution of Ca at the A-site. Further, the typical relaxor behavior of TB type ceramics has been observed in $Sr_2NaNb_5O_{15}$, $Pb_2KTa_5O_{15}$ and $Ba_5LaTi_3Nb_7O_{30}$ [16-18]. However, several works have been reported on electrical (impedance) properties of TB type compounds [19-22]. In addition, the other related tetragonal tungsten type phases $(Ba/Sr/Ca/La)_{0.6}M_xNb_{1-x}O_{3-\delta}$ (M=Mg, Ni, Mn, Cr, Fe, In, Sn) has been reported and used as anode

* Corresponding author.
E-mail: banarjibehera@gmail.com

materials for Solid Oxide Fuel Cell [23]. Moreover, structural, dielectric and ac conductivity study of $LiSr_2Nb_5O_{15}$ has already been reported by our group elsewhere [24]. Detail literature survey shows that no work has been reported on the electrical properties of $LiSr_2Nb_5O_{15}$ compound. In the present work, we report the extensive study to explore the impedance properties of LSN compound.

2 Experimental

The polycrystalline sample of $LiSr_2Nb_5O_{15}$ (LSN) was prepared by a mixed oxide method at high temperature using high-purity (99.9%) ingredients (all from M/s. Loba Chemie Pvt. Ltd., India); Li_2CO_3, Sr_2CO_3, and Nb_2O_5 in a suitable stochiometry. The oxides and carbonates were thoroughly mixed by agate mortar; first in an air atmosphere for 1 h, and then in alcohol for 1 h. The mixed powders were calcined at an optimized temperature of 950 ℃ for 7 h. The calcined powder was cold pressed into cylindrical pellets of 10 mm diameter and 1-2 mm of thickness at a pressure of 4×10^6 N/m^2 using a hydraulic press. PVA (polyvinyl alcohol) was used as binder to reduce the brittleness of the pellet, which was burnt out during the sintering. Then the pellets were sintered at an optimize temperature of 1100 ℃ for 10 h in an air atmosphere. To study the electrical/impedance properties of the compound, the sintered pellets were electroded with air-drying conducting silver paste. After electroding, the pellets were dried at 150 ℃ for 4 h to remove moisture, if any, and then cooled to room temperature before taking any measurement. The impedance parameters were obtained using an LCR meter (HIOKI Model 3532) in the frequency range of 10^2-10^6 Hz at different temperature (28-500 ℃) in conjunction with a laboratory-made sample holder and heating arrangement with an ac signal. A chromel-alumel thermocouple and a digital multimeter (M/s. Electronic of India, DM 6108) were used to measure the temperature. All the above measurements were recorded within a small temperature interval (≈2 ℃) in the heating mode.

3 Results and discussion

3.1 Impedance analysis

Complex Impedance spectroscopy [25] is a powerful technique for the characterization of electrical behavior of ceramic materials. The output response, when plotted in a complex plane, appears in the form of a succession of semicircle representing electrical phenomena due to bulk, grain boundary effect and interfacial phenomena. A polycrystalline material usually gives the grain and grain boundary properties with different time constant in two successive semicircles. The complex impedance parameters are expressed as complex impedance (Z^*) and electric modulus (M^*), complex dielectric constant (ε^*) i.e., $Z^*=Z'-jZ''$, $M^*=M'+jM''$, $\varepsilon^*=\varepsilon'-j\varepsilon''$ and tan $\delta=\varepsilon''/\varepsilon'$ where (Z', M') and (Z'', M'') are the real and imaginary components of the impedance and modulus, respectively, $j=(-1)^{1/2}$ the imaginary factor and ω is angular frequency, ($\omega=2\pi f$).

Figure 1 shows the variation of real (Z') part of impedance as the function of frequency at various temperatures (350-450 ℃). It is found that the magnitude of Z' decreases with the increase in both frequency as well as temperature (i.e., NTCR behavior). The Z' value for the selected temperature found to be merge above 10 kHz, which may be due to release of space charge of the compound with rise in temperature. The coincidence of the Z' value at higher frequency side at all the temperature confirms the concept of space charge effect [26].

Argand diagram (Z'' vs Z') at selected temperatures (350-450 ℃) is shown in Fig. 2. A single semicircular arc has been observed in selected temperature range which confirms the electrical properties of the materials arise mainly due to the contribution of bulk effect only and can be explained by a parallel RC

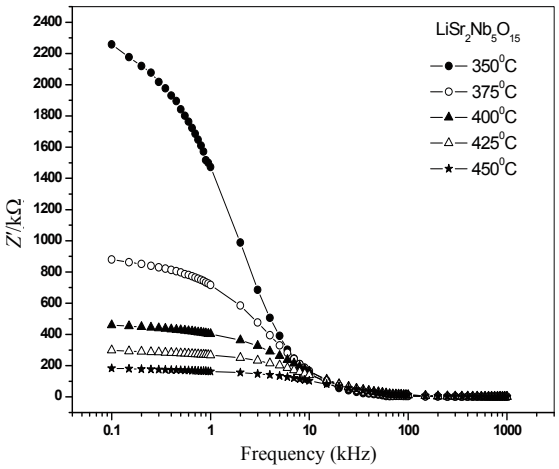

Fig. 1 Variation of Z' with frequency at different temperatures.

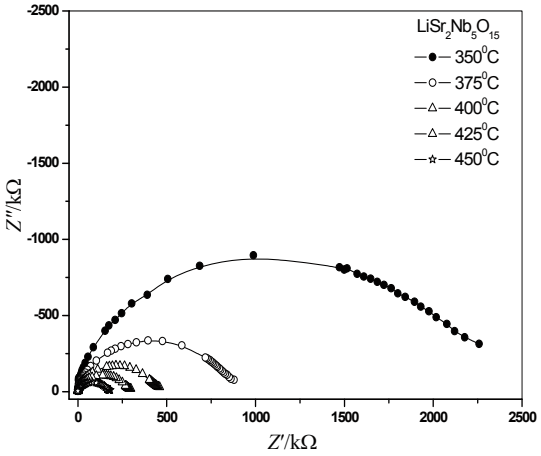

Fig. 2 Nyquist plot (Z' and Z'') at various temperatures.

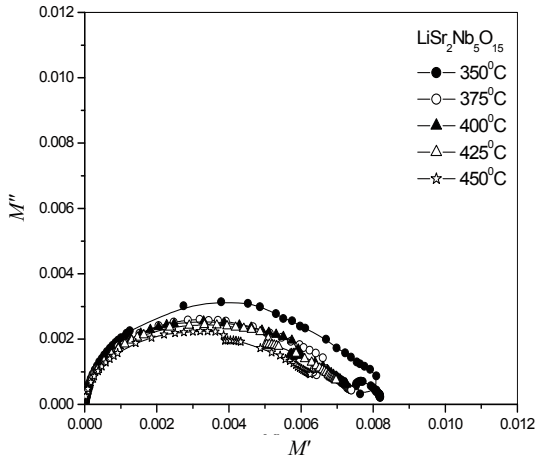

Fig. 3 Variation of (M' vs M'') at various temperature.

equivalent circuit (inset). On increasing temperature the point of intersection of semicircle on the real axis shift towards the origin of the complex impedance spectrum indicating the decrease in the resistive properties of the compound. Further, these semicircles have their center on the line below the real x-axis, indicating the departure from ideal Debye behavior (non Debye type) [27]. The calculated values of bulk resistance (R_b), relaxation frequency (f_r) and bulk capacitance (C_b) above 350 ℃ were obtained from the intercept of the semicircular arcs on real axis (shown in Table 1).

3.2 Modulus studies

In order to confirm the ambiguity arising in connection with the presence of grain/grain boundary effects at elevated temperatures, the impedance data have been re-plotted in the modulus formalism at high temperatures as shown in Fig. 3. It is clear that the modulus planes shows a single semicircle and confirm the contribution of bulk effect only.

The variation of real part of electric modulus (M') with frequency at selected temperature is shown in Fig. 4. A very low value of M' almost zero in the low frequency region, and a continuous increase in frequency having a tendency to saturate at a maximum asymptotic value in the high frequency region for all temperatures. This is attributed to the presence of conduction phenomena due to short range mobility of charge carriers.

Table 1 Values of bulk resistance (R_b), relaxation frequency (f_r) and bulk capacitance (C_b) of $LiSr_2Nb_5O_{15}$ compound at different temperature

T (℃)	R_b (kΩ)	f_r (kHz)	C_b (pF)
350	2452.74	2	32
375	910.7	4	44
400	474.75	7	48
425	296.04	10	54
450	193.36	15	55

Variation of Z'' and M'' with frequency at various temperatures is shown in Fig. 5. Both the peaks of the plots for Z'' and M'' are shifted towards the higher frequency on increasing temperature. The change in the peak broadening (Z'' vs. frequency) on the change of temperature suggests the presence of temperature dependent relaxation process. This is due to the presence of some immobile electrons or species

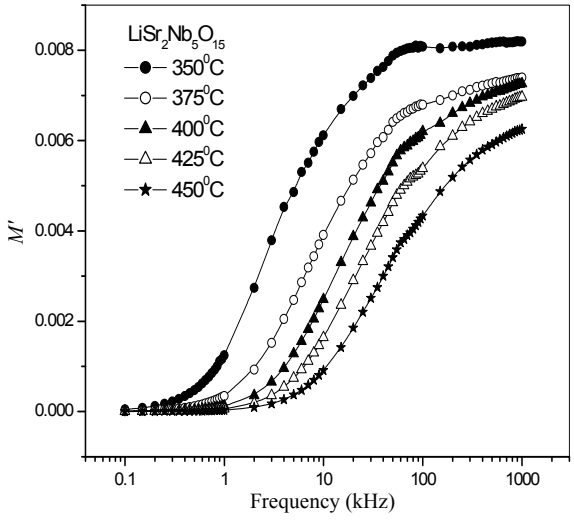

Fig. 4 Variation of M' with frequency at different temperature.

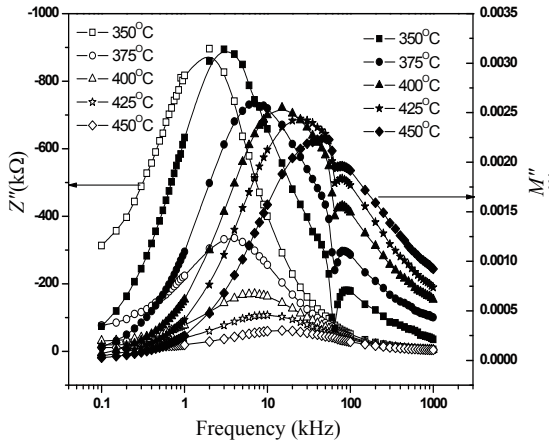

Fig. 5 Variation of Z'' and M'' with frequency at different temperatures.

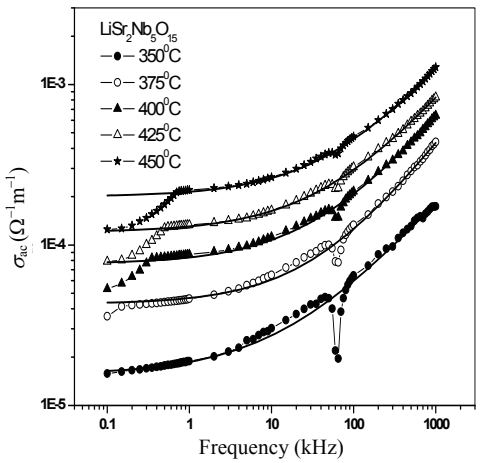

Fig. 6 Frequency dependence of ac conductivity at different temperature.

present at low temperature and defects created at high temperature [28]. Finally, all the curves for Z'' merge at high frequency due to the accumulation of space charge. The behavior (M'' vs. frequency) suggests the dielectric relaxation is thermally activated in which the hopping mechanism of charge carriers dominates intrinsically in the compound. The asymmetry in peak broadening as observed in M'' plot shows the spread of relaxation times with different time-constant, and confirms the relaxation is of non-Debye type (also observed from Nyquist plot).

3.3 Conductivity studies

Figure 6 shows frequency dependence of ac conductivity (σ_{ac}) at various temperatures. It is observed that at low frequencies and high temperatures the plateaus of (σ_{ac}), i.e., frequency independent values of conductivity, which corresponds to the dc conductivity. This can be described by a relation $\sigma(\omega)=\sigma_{dc}+A\omega^n$ known as Jonscher's universal power law [29], where A is the temperature dependent parameter and n is the temperature dependent exponent. The term $A\omega^n$ comprises the ac dependence and characterizes all dispersion phenomena. The exponent n can vary from material to material, but in general it can have values between 0 to 1 ($0 \leqslant n \leqslant 1$). This is confirmed by a typical fit of the above equation with the experimental data. The solid lines (Fig. 6) are the fitted lines. The values of fitted parameters are shown in Table 2. The values of n lie in the range of 0.57-0.67 (350-450 ℃). According to Jonscher, the frequency at which slope changes, is known as hopping frequency (ω_p). This behavior suggests the presence of hopping mechanism between the allowed sites. The conductivity between 375 ℃ to 450 ℃ exhibit a step like decrease on low frequency side may be due to transition from the bulk to a contact resistance [15]. Moreover, the dc conductivity values obtained from the fitted parameters are nearly equal to the values (shown in the Table 2) obtained from Fig. 7. An anomaly observed near 100 kHz may be due to the onset of the conductivity relaxation, which indicates the translation from long range hopping to the short range ion motion [30] similar to M'' with frequency.

Figure 7 shows the variation of dc (bulk) conductivity with inverse of temperature ($10^3/T$). The dc conductivity was evaluated from the complex impedance plots at different temperatures. It is observed that the dc conductivity increases with rise in

Table 2 Fitting parameters obtained from Jonscher's power law at different temperatures. Comparison between the dc conductivity obtained from fitted parameters and from Fig. 6 (in parenthesis)

T (℃)	σ_{dc} ($\Omega^{-1}m^{-1}$)	A	n	Goodness of fit (R^2)
350	0.00002 (1.68737E-5)	5.5897E-9	0.5793	0.999
375	0.00004 (3.76853E-5)	3.6306E-8	0.6720	0.997
400	0.00008 (7.19290E-5)	9.4667E-8	0.6288	0.997
425	0.00012 (1.22885E-4)	1.5623E-7	0.5829	0.996
450	0.00020 (1.88141E-4)	2.0148E-7	0.6207	0.994

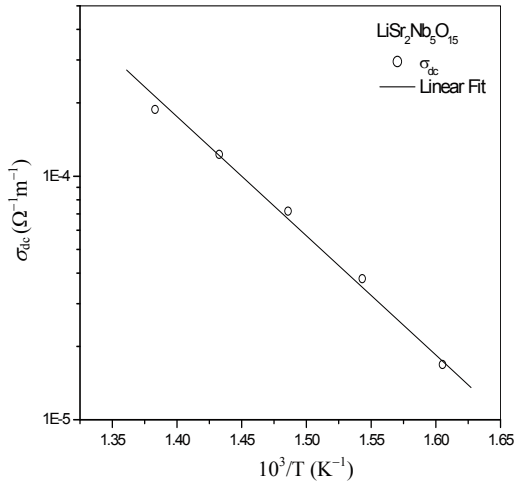

Fig. 7 Variation of dc conductivity with inverse of temperature.

temperature showing a typical characteristic of a semiconductor i.e., NTCR behavior. From this plot a straight line is observed and follows the Arrhenius law (since the electrical conductivity is thermally activated process): $\sigma_{dc}=\sigma_0\exp(-E_a/k_BT)$, where σ_o is the pre-exponential term and E_a is activation energy. The activation can be calculated from the slope of the straight line and found to be 0.97 eV. This amount of energy is required for the conduction process of the material.

4 Conclusions

The polycrystalline sample of $LiSr_2Nb_5O_{15}$ (LSN) was prepared by a high temperature solid state reaction technique. X-ray analysis exhibits the orthorhombic crystal structure at room temperature [24]. Complex impedance spectroscopy was used to study the electrical properties of the material. The complex impedance plot reveals the contribution of bulk effects only and the bulk resistance decreases with rise in temperature which shows NTCR behavior. The relaxation process occur in the compound has been found to be temperature dependent. The ac conductivity spectrum is found to obey Jonscher's universal power law. Variation of dc conductivity (bulk) with temperature exhibits Arrhenius type of electrical conductivity and the activation energy for conduction process is found to be 0. 97 eV.

Acknowledgement

The authors (PN and BB) acknowledge the financial support through DRS-I under SAP of UGC for the development of research work in the School of Physics, SU.

References

[1] Jamieson PB, Abrahams SC, Bernstein JL. Ferroelectric tungsten bronze-type crystal structures. I. Barium strontium niobate $Ba_{0.27}Sr_{0.75}Nb_2O_{5.78}$. *J Chem Phys* 1968, **48**: 5048-5057.

[2] Uchino K. Electrooptic ceramics and their display applications. *Ceram Inter* 1995, **21**: 309-315.

[3] Neurgaonkar RR, Oliver JR, Nelson JG. Piezoelectric and ferroelectric properties of La-modified and unmodified tungsten bronze $Pb_{0.6}Ba_{0.4}Nb_2O_6$ dense ceramics. *Mater Res Bull* 1991, **26**: 771-777.

[4] Venturini EL, Spencer EG, Ballman AA. Elasto - optic properties of $Bi_{12}GeO_{20}$, $Bi_{12}SiO_{20}$, and $Sr_xBa_{1-x}Nb_2O$. *J Appl Phys* 1969, **40**: 1622-1966.

[5] Sakamoto S, Yazaki T. Anomalous electro-optic properties of ferroelectric strontium barium niobate and their device applications. *Appl Phys Lett* 1973, **22**: 429-431.

[6] Geusic JE, Levinstein HJ, Singh S, *et al*. Continuous o.532-μ, solid-state source using $Ba_2NaNb_5O_{15}$. *Appl Phys Lett* 1968, **12**: 306-308.

[7] Sholokhavich ML, Dugin EV, Rybina IN. Solid-state synthesis of ferroelectric lead metatantalate. *Inorg Mater* 2001, **37**: 405-407.

[8] Hornebecq V, Elissalde C, Weill FA, *et al*. Wide frequency range dispersion and relaxations in ceramics of the $K_6Li_4Ta_{10}O_{30}$-$Pb_5Ta_{10}O_{30}$ system. *J Ravez Phys Status (a)* 1998, **169**: 311-320.

[9] Hornebecq V, Elissalde C, Reau JM, *et al*. Relaxations in new ferroelectric tantalates with tetragonal tungsten bronze structure. *Ferroelectrics* 2000, **238**: 57-63.

[10] Bijumon PV, Kohli V, Prakash O, *et al*. Dielectric properties of $Ba_5MTi_3A_7O_{30}$ [M=Ce, Pr, Nd, Sm, Gd, Dy and Bi; A=Nb, Ta] ceramics. *Mater Sci Eng B* 2004, **113**: 13-18.

[11] Chi EO, Gandini A, Ok KM, *et al*. Syntheses, structures, second-harmonic generating, and ferroelectric properties of tungsten bronzes: $A_6M_2M'_8O_{30}$ ($A=Sr^{2+}$, Ba^{2+}, or Pb^{2+}; $M=Ti^{4+}$, Zr^{4+}, or Hf^{4+}; $M'=Nb^{5+}$ or Ta^{5+}). *Chem Mater* 2004, **16**: 3616-3622.

[12] Xin Yin, Liu Shi, Ang Wei, *et al*. Effect of structural packing on the luminescence properties in tungsten bronze compounds $M_2KNb_5O_{15}$ (M=Ca, Sr, Ba). *J of Solid State Chemistry* 2012, **192**: 182-185.

[13] Behera B, Nayak P, Choudhary RNP. Dielectric and

impedance properties of $LiCa_2Nb_5O_{15}$ ceramics. *J Mater Sci Mater: Electron* 2008, **19**: 1005-1011.

[14] Behera B, Nayak P, Choudhary RNP. Impedance spectroscopy study of $NaCa_2Nb_5O_{15}$. *Modern Physics Letters B* 2009, **23**: 97-109.

[15] Behera B, Nayak P, Choudhary RNP. Structural and electrical properties of $KCa_2Nb_5O_{15}$ ceramic. *Cent Eur J Phys* 2008, **6**: 289-295.

[16] Torres-Pardo A, Jimenez R, Gonzalez-Calbet JM, *et al*. Structural effects behind the low temperature nonconventional relaxor behavior of the $Sr_2NaNb_5O_{15}$ bronze. *Inorganic Chem* 2011, **50**: 12 091-12 098.

[17] Sciau Ph, Lui Z, Calvarin G, *et al*. Structural study of a tungsten bronze relaxor compound $[Pb_2KTa_5O_{15}]$. *Materials Research Bulletin* 1993, **28**(12): 1233-1239.

[18] Li Kun, Zhu Xiao Li, Liu Xiao Qiang, *et al*. Relaxor ferroelectric characteristics of $Ba_5LaTi_3Nb_7O_{30}$ tungsten bronze ceramics. *Applied Physics Letters* 2012, **100**: 012902.

[19] Xie Rong-Jun, Akimune Yoshio, Matsuo Kazuo, *et al*. Dielectric and ferroelectric properties of tetragonal tungsten bronze $Sr_2A_xCa_xNaNb_5O_{15}$ (x=0.05-0.35) ceramics. *Applied Physics Letters* 2002, **80**: 835-837.

[20] Ganguly P, Jha AK, Deori KL. Investigations of dielectric, pyroelectric and electrical properties of $Ba_5SmTi_3Nb_7O$ ferroelectric ceramic. *J of Alloys and Compounds* 2009, **484**: 40-44.

[21] Bouziane M, Taibi M, Boukhari A. Synthesis and ferroelectric properties of rare earth compounds with tungsten bronze type structure. *Materials Chemistry and Physics* 2011, **129**: 673-677.

[22] Padhee R, Das PR, Parida BN, *et al*. Structural, dielectric and electrical properties of dysprosium based new complex electroceramics. *J Mater Sci: Mater Electron* 2012, **23**: 1688-1697.

[23] Slater PR, Irvine JTS. Synthesis and electrical characterization of the tetragonal tungsten bronze type phases $(Ba/Sr/Ca/La)_{0.6}M_xNb_{1-x}O_{3-\delta}$ (M=Mg, Ni, Mn, Cr, Fe, In, Sn): Evaluation as potential anode materials for solid oxide fuel cells. *Solid State Ionics* 1999, **124**: 61-72.

[24] Behera B, Mohanty NK, Satpathy SK P, *et al*. Structural and dielectric properties of $LiSr_2Nb_5O_{15}$ ceramic. *AIP Conf Proc* 2011, **1372**: 11-14.

[25] Mac Donald JR. *Impedance Spectroscopy*. John Wiley and Sons, 1987.

[26] Plocharski J, Wieczoreck W. PEO based composite solid electrolyte containing nasicon. *Solid State Ionics* 1988, **28-30**: 979-982.

[27] Sinclair DC, West AR. Effect of atmosphere on the PTCR properties of $BaTiO_3$ ceramics. *J Mater Sci* 1994, **29**: 6061-6068.

[28] Behera B, Nayak P, Choudhary RNP. Impedance spectroscopy study of $NaBa_2V_5O_{15}$ ceramic. *Journal of Alloys and Compounds* 2007, **436**: 226-232.

[29] Jonscher AK. The 'universal' dielectric response. *Nature* 1977, **267**: 673-679.

[30] Bhagat S, Prasad K. Structural and impedance spectroscopy analysis of $Ba(Fe_{1/2}Nb_{1/2})O_3$ ceramic. *Phys Status Solidi A* 2010, **207**: 1232-1239.